J. Phys. B: At. Mol. Opt. Phys. **29** (1996) 531–543. Printed in the UK

Ionization of metastable neon by electron impact

M Johnston, K Fujii, J Nickel and S Trajmar

Department of Physics, University of California, Riverside, California 92521, USA

Received 13 June 1995, in final form 3 November 1995

Abstract. The partial electron impact ionization cross section for metastable neon, Ne^{*+}, has been measured in the energy range from threshold to 200 eV. The crossed-beam experiment used a fast neutral target (both ground state and ground state plus metastable) formed by charge transfer between an 800 eV neon ion beam and neon gas or sodium vapour. The ionization cross section for the $^3P_2$ and $^3P_0$ metastable components, which are assumed to be equal, was placed on an absolute scale by utilizing the known ground-state cross section and assuming that the beam fractions of the mixed state were statistically distributed. The results are compared with previous experimental and theoretical work.

1. Introduction

Because of their capacity to store energy and their long lifetimes, metastable rare gas atoms play important roles in a wide variety of physical systems such as laboratory plasmas, lamps, and laser discharges. For example, in rare gas laboratory plasmas metastable atoms are important in maintaining the discharge. In a typical rare gas plasma, the relative density of metastable to ground-state atoms is 10^{-4}, while the degree of ionization with respect to the ground-state population is only 10^{-5}. The relatively large population of metastables combined with their large cross sections in electron impact processes makes them an efficient intermediary for stepwise excitation and ionization in rare gas discharges, and knowledge of the corresponding cross sections is important for modelling these discharges (Makabe *et al* 1992, Sommerer and Kushner 1992, Lymberopoulos and Economou 1993). In rare gas excimer lasers, metastable rare gas atoms are active in non-equilibrium chemistry which leads to population inversion in the laser media (Cartwright 1993, Jacob and Mangano 1976, Daugherty *et al* 1976).

While electron collision processes involving metastables are of interest for both practical and theoretical reasons, the measured cross section database is sparse (Lin and Anderson 1991, Trajmar and Nickel 1993). Table 1 shows the available data for ionization of rare gas metastables by electron impact. Most of the work has been done on helium, and, with the exception of Dixon *et al* (1973, 1976), most of the work has been over a limited electron impact energy range. One reason for this paucity is the formidable task of producing a well-characterized metastable beam of sufficient density to carry out the collision experiments.

We have constructed an apparatus for producing fast metastable beams (800 eV) and for measuring various electron impact cross sections for the metastable rare gases. The results of our first experiment, the electron impact ionization cross sections for metastable neon, are presented here. Neon was chosen as the first species for practical reasons which are discussed later.

0953-4075/96/030531+13$19.50

Table 1. A summary of available data for ionization of metastable rare gases by electron impact.

Gas	Investigation	Ionization potential (Moore 1971)	Energy range (eV)
Helium	Fite and Brackmann (1963)	$^1S_0 = 24.580$ eV	3–24
	Vriens *et al* (1968)	$2\,^3S_1 = 4.766$ eV	3–18
	Koller (1969)	$2\,^3S_0 = 3.970$ eV	5–12
	Long and Geballe (1970)		5–16
	Dixon *et al* (1973, 1976)		6–1000
	Shearer-Izumi and Botter (1974)		3–23
	Baum *et al* (1989)		4.8–24.6
Neon	Dixon *et al* (1973) not published	$^1S_0 = 21.559$ eV	5.6–500
		$3\,^3P_2 = 4.944$ eV	
		$3\,^3P_0 = 4.848$ eV	
Argon	Dixon *et al* (1973) not published	$^1S_0 = 15.755$ eV	5.6–500
		$4\,^3P_2 = 4.210$ eV	
		$4\,^3P_0 = 4.035$ eV	
Krypton	None	$^1S_0 = 13.996$ eV	
		$5\,^3P_2 = 4.083$ eV	
		$5\,^3P_0 = 3.436$ eV	
Xenon	None	$^1S_0 = 12.127$ eV	
		$6\,^3P_2 = 3.814$ eV	
		$6\,^3P_0 = 2.682$ eV	

In section 2 we describe the experimental apparatus and in section 3 discuss the extraction of the cross section from the experimental signal and the problems inherent in a mixed-initial-state crossed-beam experiment. The results are presented in section 4 and our conclusions are given in section 5.

2. Experimental apparatus

An overall schematic diagram of the apparatus is shown in figure 1. A neon ion beam with a kinetic energy of 800 eV is extracted from a neon plasma source and is transported by a periodic focusing electrostatic lens system 16.25 cm through the source chamber, typically at 7×10^{-5} Pa, to a charge exchange cell. The periodic focusing system is based on the ideas of Pierce (1954). Transporting the beam reduces the plasma source gas load in the interaction region. Typical pressure in the interaction region is 7×10^{-8} Pa with the source running. The charge exchange cell can be filled with either the parent neon gas or with sodium vapour. When the cell is filled with neon gas, the ion beam is resonantly converted through charge exchange into a neutral ground-state beam. When the cell is filled with sodium vapour, the neon ions are resonantly neutralized into the excited 3s manifold. The $2p^5 3s\,^3P_{0,2}$ levels are metastable while the $2p^5 3s\,^3P_1$ and $2p^5 3s\,^1P_1$ levels radiatively decay to the ground state. Thus, with a sodium vapour charge transfer target, the emerging neon beam is composed of a mixture of ground-state and metastable species. When the levels in the 3s manifold are populated in proportion to their statistical weight during the charge exchange process, the resulting neutral beam consists of 50% ground-state species, 42% $3s\,^3P_2$ species and 8% $3s\,^3P_0$ species. Both Neynaber and Magnuson (1977) and Coggiola

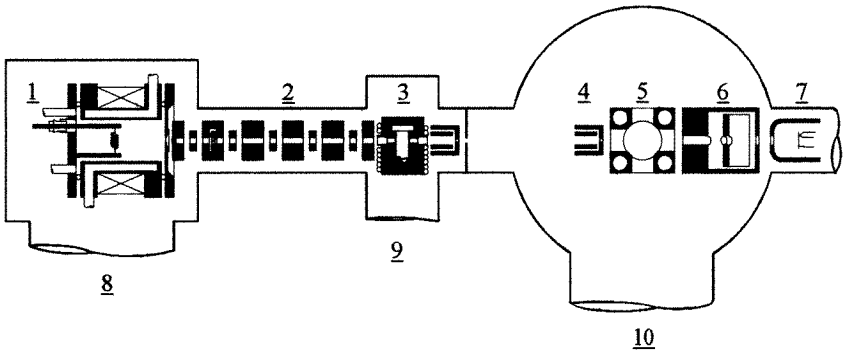

Figure 1. Overview of metastable ionization apparatus: (1) plasma ion source, (2) periodic focusing lens train, (3) charge exchange cell and ion deflectors, (4) ion deflectors, (5) electron gun, (6) parallel-plate ion detector, (7) thermoelectric neutral detector, (8) port to Edwards Diffstak CR250/2000P diffusion pump, (9) port to Edwards Diffstak 63/150P diffusion pump, (10) port to Varian UHV-8 cryo pump.

et al (1979) found this to be the case for neon.

Following the 1 cm long charge exchange cell, a set of deflectors produce an electric field of 3700 V cm^{-1} to ionize Rydberg atoms produced in the charge exchange cell and remove any remaining charged particles from the beam. Conservative calculations show that Rydberg atoms with $n \geqslant 18$ are ionized by the electric field. Rydberg atoms with $n \leqslant 7$ decay before they enter the interaction region. To test for Rydberg atoms in the neutral particle beam, cross sections were measured with and without the deflectors on. No differences were observed in the measured cross sections. With a 0.032 Pa sodium vapour charge transfer target, the typical neutral neon flux leaving the charge exchange cell was 10^{16} neutrals s^{-1} Sr measured by a thermoelectric neutral particle detector. This corresponds to a neutral density of 10^6 neon metastables cm^{-3} and 10^6 neon ground states cm^{-3} in the UHV interaction region 23 cm away.

The thermoelectric neutral particle detector is a hybrid of thermal and secondary electron emission techniques based on the ideas of Chambers (1964). As a neutral beam strikes the surface of a negatively biased plate, electrons are ejected and heat is transferred to the detector. The ratio of the ejected electron current to the incident neutral particle current is the secondary emission coefficient, δ, given by

$$\delta = \frac{I_s}{I_n} \tag{1}$$

where I_s is the secondary emission current, and I_n is the neutral particle beam current.

If the detector plate has an initial temperature T_0 and a current is applied, the temperature will rise asymptotically to some temperature T_f. The temperature change, $\Delta T = T_f - T_0$, is proportional to the incoming current at a fixed beam energy. Comparison of the temperature change due to an ion beam of known current and the same energy as the neutral particle beam calibrates the detector. The ion current is measured by biasing the detector to collect secondary electrons, and using it as a Faraday cup.

Once the thermal properties of the detector are known, it can be used to determine the particle current in a neutral beam of known energy. The secondary emission coefficient, δ, is determined by comparing the particle current with the secondary emission current. With knowledge of δ for the surface of the detector, measurements of the neutral particle current are possible by monitoring the secondary emission current. Because δ is very sensitive to

the surface conditions of the detector, recalibration is necessary after any change to the system that could affect surface conditions on the detector, such as deposition of sodium from the charge exchange cell. The resolution of the detector is better than 1×10^{-4} °C with a time constant of about 3 min. The practical limit on beam power resolution is 0.1 μW which corresponds to a current of 0.13 nA measured with an 800 eV neutral neon beam.

It must be emphasized that the thermoelectric detector measures only the total current of the neutral beam, while in the ionization experiment the relevant parameter is the neutral beam density in the interaction region. A knowledge of the beam geometry together with the total beam current allows the density to be inferred at any position along the beam. Fortunately, in our case, absolute densities are never required, but only ratios of mixed states to ground-state densities. In this case the geometrical factors cancel out so that ratios of currents are proportional to ratios of densities. Detailed descriptions of both the metastable source and the thermoelectric neutral detector are the subjects of soon to be submitted papers.

The UHV interaction chamber is separated by a 2.5 mm aperture from the source chamber. At the centre of the UHV chamber, the neutral beam is crossed with a variable energy, magnetically collimated electron beam, forming the interaction for the ionization experiment, see figure 1. The fast neutral beam is defined by a 2.5 mm aperture located immediately in front of the interaction region and 23 cm from the charge exchange cell. A set of deflectors just upstream from the beam defining aperture removes any ions generated by stripping of fast neutrals with background gas between the conversion cell and the interaction region. Ions produced in the interaction region (as well as stripped ions) are removed from the beam by the parallel plate detector and are detected by a channeltron detector. The ionization experiment is carried out in a UHV chamber to minimize the noise signal produced by stripping of the fast neutral beam with background atoms.

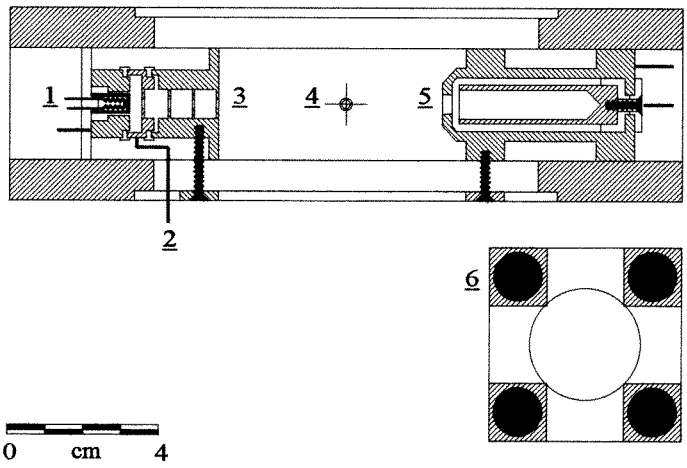

Figure 2. Magnetically collimated electron gun and Faraday cup: (1) indirectly heated barium scandate cathode, (2) aperture A_1, anode, (3) aperture A_2, (4) interaction region, (5) Faraday cup, (6) permanent magnets.

A schematic diagram of the electron gun is shown in figure 2. The electrons are emitted from an indirectly heated barium scandate cathode and an anode, formed by aperture, A_1, is biased at a potential $V_1 - V_0$ with respect to the cathode, where V_0 and V_1 are measured with respect to ground. The extraction bias is typically 20–25 V. The beam energy is set by

$E = V_2 - V_0$, where V_2 is the potential of aperture A_2. In practice, V_2 is held at ground or tank potential, and $V_0 = -E$. The impact energy, E, is typically swept between 0–200 V. The electron beam is confined by an axial magnetic field of about 140 G produced by four cast Alnico grade 5 permanent magnets placed parallel to the beam. The electron beam current is collected at the Faraday cup and is measured by a Keithley 485 picoammeter. The analogue output of the picoammeter goes to a voltage-to-frequency converter before being sent to a Nuclear Data model ND62 multichannel scaler. The ND62 ramp output is used to control the impact energy through a Kepco programmable PCX 100 power supply so that the Faraday cup current can be monitored as a function of the electron impact energy. By most measures, the electron gun-Faraday cup system appears to work well. The electron gun current has an onset at about 1–2 eV (measured applied E) impact energy, rapidly rises to a maximum value which can be adjusted from 0–500 μA, and operates stably for hours. However, there are some inherent properties of magnetically collimated guns which can be detrimental in crossed-beam experiments. First, the beam formed in a magnetically collimated gun does not have a constant radius but has a 'sausage-link-like' shape along its length, with a maximum radius r_{max}, and a minimum radius r_{min}, which vary in magnitude and axial position with the beam current and energy (Septier 1967). Thus the overlap geometry between the neutral and electron beams can be electron-energy dependent, causing artificial structures in the cross section measurement which we have seen. To avoid these effects, the atomic beam must be larger than the maximum radius of the electron beam. Also, at low impact energies and practical electron beam currents, the electron beam has a high pervasion and the kinetic energy of electrons in the interaction region may be lower than that inferred from an external measurement of E. Furthermore, the magnitude of this depression is a complicated, unknown function of E so that a simple offset correction to the energy scale cannot be rigorously applied. To minimize these effects, the maximum electron current should be as low as possible, consistent with adequate signal to noise conditions. Our maximum currents were in the 10–20 μA range where the effects are estimated to be less than 250 meV up to beam energies of 20 eV and less than 100 meV above 20 eV.

Ions generated in the interaction region, the ion signal, are separated from the main neutral beam and detected by the parallel-plate analyser shown in figure 3. The parallel plates are oriented at 45° with respect to the ion beam axis and are separated by 1.35 cm. The entrance and exit apertures have diameters of 0.5 cm and 1 cm, respectively, and 0.8 cm diameter holes in the back parallel plate and housing allow the neutral beam to pass through the analyser to the thermoelectric neutral detector. An analysis using the SIMION electrostatic design program developed by the Idaho National Engineering Laboratory correctly predicted that the einzel lens shown in figure 3 would increase the transmission of ion current to the channeltron. The lens is made up of three cylindrical elements, 3.6 mm long, with inner diameters of 10 mm separated by gaps of 1 mm. The two outer elements are grounded while the centre element operates at 600 V. The entire parallel-plate analyzer system is enclosed in an aluminum housing which also contains the Galileo Electro-Optics No 4039 channeltron. While not directly relevant to our measurement, we used an incident ion beam to determine that the overall collection efficiency of the parallel-plate detector is about 25%.

3. Extraction of ionization cross sections from the ion signal

When the neon ion beam is neutralized in sodium vapour, the resulting beam is ultimately made up of a ground state (^{1}S) and two metastable ($3s\,^3P_2$, $3s\,^3P_0$) components. This mixed initial state complicates the direct measurement of individual cross sections, as can be seen by the following example. Let $\sigma_g(E)$, $\sigma_1(E)$ and $\sigma_2(E)$ be the electron impact ionization

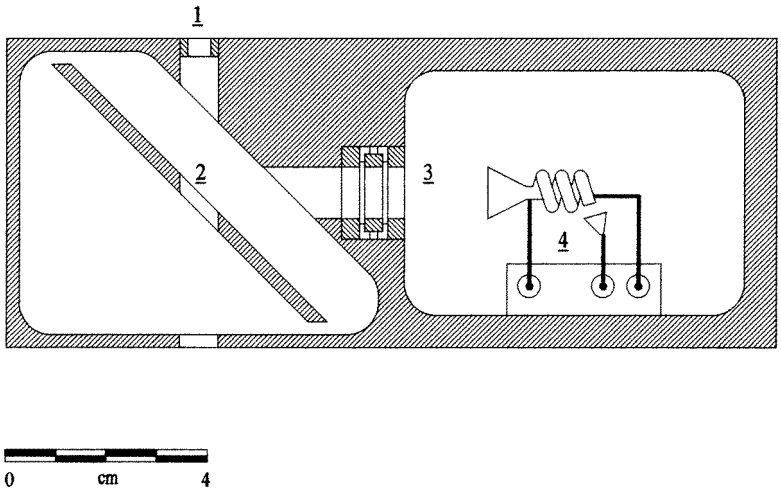

Figure 3. Parallel-plate ion detector: (1) entrance aperture, (2) parallel plate, (3) einzel lens, (4) channeltron.

cross sections out of the ground state and the two metastable levels. The subscript 1 denotes the $^3P_2$ species and the subscript 2 denotes the $^3P_0$ species. In the interaction region, let the density of the ground-state atoms be n_g and the densities of the two metastable species be n_1 and n_2. The total neutral density is then given as $n_0 = n_g + n_1 + n_2$. The ion production rate can be written

$$\dot{N}_{ion}(E) = \eta l \frac{I_e}{e}(n_g\sigma_g(E) + n_1\sigma_1(E) + n_2\sigma_2(E)) \tag{2}$$

where η is the detection efficiency, l is the effective scattering length travelled by the electron beam, and I_e is the electron current. It is useful to define the metastable beam fractions as $f_g = n_g/n_0$, $f_1 = n_1/n_0$, and $f_2 = n_2/n_0$. Equation (2) can then be written as

$$\dot{N}_{ion}(E) = \eta l \frac{I_e}{e} n_0\sigma_w(E) \tag{3}$$

where the weighted cross section, σ_w, is given by

$$\sigma_w(E) = ((1 - f_1 - f_2)\sigma_g(E) + f_1\sigma_1(E) + f_2\sigma_2(E)). \tag{4}$$

It is seen from equation (3) that a single experimental measurement at energy E can at most determine the weighted cross section, σ_w. To extract further information from σ_w, σ_g and the beam fractions need to be known. We can then infer the average quantity $\sigma_{12} = f_1\sigma_1 + f_2\sigma_2$. Thus a single measurement yields only the average quantity σ_{12}. In order to obtain σ_1 and σ_2 individually, two experiments need to be performed on neutral beams having (preferably widely) different beam fractions f_1 and f_2. Ideally, two experiments could be performed in which f_1 and f_2 are alternately made zero, say by laser pumping (but while the laser pumping procedure is suitable for thermal mixed beams, it proved impractical for our fast beam arrangement). For the results reported here, the beam fractions have been determined by the statistical weights argument, and it has been assumed that $\sigma_1 = \sigma_2$. We can treat σ_1 and σ_2 in the same way because the cross section for ionization out of a given configuration depends on the orbital of the excited electron. For a given excitation, $^3P_2$ and $^3P_0$ cross sections are different, however, in ionization the angular information 'drops' out and the cross sections are the same for a given configuration. This is supported by distorted wave

approximation (DWA) calculations made at Los Alamos National Laboratories by Clark and Mann (Csanak *et al* 1995).

As equation (3) shows, the product ηl needs to be known in order to determine σ_w. In reality, l is obtained from a complicated unknown overlap integral, but the following arguments remain unchanged. To determine ηl, neon gas is placed in the charge exchange cell to generate a ground-state fast neutral beam and a ground-state ionization experiment is performed. Inherent in this technique is the assumption that ηl is the same for the ground-state and mixed-species beams. This is justified because the beams are well collimated and have energies of 800 eV. Any difference in energies between the two beams that would give rise to different detection efficiencies are extremely small and will not effect η.

At the fixed electron impact energy E', ηl is given by

$$\eta l = \frac{e}{I_e^{gb}(E')} \frac{1}{n_0^{gb}\sigma_g} \dot{N}_{ion}^{gb}(E') \tag{5}$$

where gb, refers to a ground-state beam measurement and n_0^{gb} is the ground-state beam neutral density. Combining equations (3) and (5), we have

$$\sigma_w(E) = \frac{\dot{N}_{ion}^{mb}(E)}{\dot{N}_{ion}^{gb}(E')} \frac{n_0^{gb}}{n_0^{mb}} \frac{I_e^{gb}(E')}{I_e^{mb}(E)} \sigma_g(E') \tag{6}$$

where the superscript mb refers to the mixed-state beam and E' is the fixed electron impact energy of the ground-state measurement, which in our case was 90 eV. The ion count rates and the electron currents can be measured individually and the ratio of the neutral densities can be determined from the thermoelectric detector measurements. The metastable ionization cross sections $\sigma_1 = \sigma_2 = \sigma_m$ can thus be extracted using the statistical weights assumptions stated above.

The data acquisition employed the following sequential procedures. First, neon gas was admitted to the charge exchange cell to generate a fast ground-state neutral beam and the ionization signal was acquired by sweeping E from 0–200 eV. The sweeping was arranged so that only the background (electron gun off) was collected by the MCS (multichannel scaler) on the first half of the sweep cycle, and the signal-plus-background was collected during the second half of the cycle. After correcting for background, energy dependence of the electron gun current, and adjusting the energy scale, the ground-state ionization data were fitted to the shape of the ground-state data of Krishnakumar and Srivastava (1988), with the quality of the fit taken as an indicator of proper operation of the apparatus.

Next, the energy of the electron gun was set to $E' = 90$ eV and the ion count rate, $\dot{N}_{ion}^{gb}(E') = [(\text{signal plus background}) - (\text{background})]$, the electron current $I_e^{gb}(E')$, and the secondary emission current due to the neutral beam I_s^{gb}, were measured. Then δ^{gb} for the ground-state beam was measured using the thermoelectric detector. The neon was then removed from the charge exchange cell. The charge exchange cell was then heated to introduce sodium vapour for generating a mixed-states beam. All beam tuning parameters remain constant during this transition which takes ~ 1 h. Once the mixed states beam was stable, the secondary emission coefficient for the mixed states beam, δ^{mb}, was determined. With the electron energy set at $E' = 90$ eV the count rate, $\dot{N}_{ion}^{mb}(E')$, the electron current $I_e^{mb}(E')$, and the secondary emission current, I_s^{mb}, for the mixed-states beam were measured, setting the absolute scale of the weighted cross section. Next, the energy of the electron gun was swept from 0–200 eV and the shape of the weighted cross section and the electron current profile were obtained as in the ground-state case. During the ionization signal acquisition, the neutral beam current is monitored by sampling the secondary electron

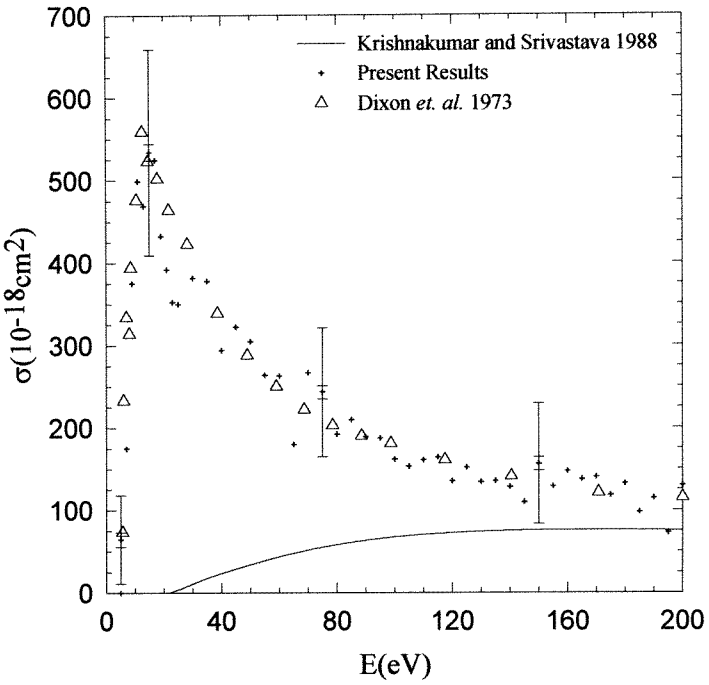

Figure 4. Partial electron impact ionization cross section of metastable neon, Ne^{*+}, compared with previous experimental results of Dixon *et al* (1973) and the experimental results for the partial electron impact ionization of ground-state neon, Ne^{+}, of Krishnakumar and Srivastava (1988). The outer limits on the error bars give the total error, systematic and statistical, while the inner limits give the statistical error.

current from the thermoelectric detector so that minor corrections for neutral beam drift can be made.

The weighted cross section, $\sigma_{\mathrm{w}}(E)$, can be calculated from equation (7):

$$\sigma_W(E) = \left[\frac{\dot{N}^{\mathrm{mb}}_{\mathrm{ion\ shape}}(E)}{I^{\mathrm{mb}}_{\mathrm{e\ shape}}(E)}\right]\left[\frac{I^{\mathrm{mb}}_{\mathrm{e\ shape}}(E')}{\dot{N}^{\mathrm{mb}}_{\mathrm{ion\ shape}}(E')}\right]\left[\frac{\dot{N}^{\mathrm{mb}}_{\mathrm{ion}}(E')}{I^{\mathrm{mb}}_{\mathrm{e}}(E')}\frac{\delta^{\mathrm{mb}}}{I^{\mathrm{mb}}_{\mathrm{s}}(E')}\right] \times \left[\frac{I^{\mathrm{gb}}_{\mathrm{e}}(E')}{\dot{N}^{\mathrm{gb}}_{\mathrm{ion}}(E')}\frac{I^{\mathrm{gb}}_{\mathrm{s}}(E')}{\delta^{\mathrm{gb}}}\right]\sigma_{\mathrm{g}}(E') \tag{7}$$

where the first two bracketed terms give a shape normalized at 1 at the energy E' and the other terms set the absolute scale at the energy E' relative to the experimental results for $\sigma_{\mathrm{g}}(E')$ of Krishnakumar and Srivastava (1988). Using equation (4) the metastable cross section was then calculated, based on our assumptions that $\sigma_{\mathrm{m}}(E) = \sigma_1(E) = \sigma_2(E)$, that $f_{\mathrm{g}} = 0.5$, $f_1 = 0.42$, and $f_2 = 0.08$ and the ground-state data of Krishnakumar and Srivastava. From equations (4) and (7) we see that the shape of $\sigma_{\mathrm{m}}(E)$ depends on the shapes of $\sigma_{\mathrm{w}}(E)$ and $\sigma_{\mathrm{g}}(E)$ and the absolute scale of $\sigma_{\mathrm{w}}(E)$ depends on known ground-state data at E', $\sigma_{\mathrm{g}}(E')$. We measure $\sigma_{\mathrm{w}}(E)$ and rely on the results of Krishnakumar and Srivastava for $\sigma_{\mathrm{g}}(E')$ and $\sigma_{\mathrm{g}}(E)$.

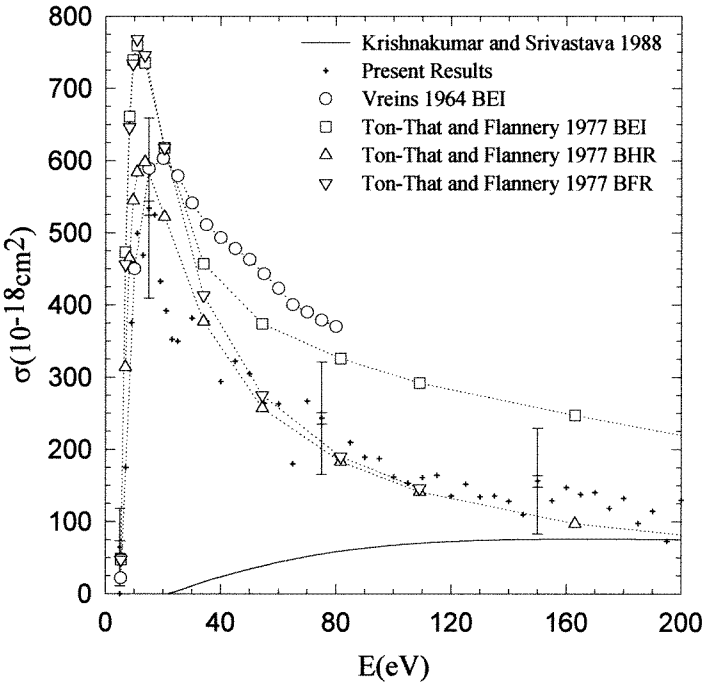

Figure 5. Present results for the partial electron impact ionization cross section of metastable neon, Ne^{*+}, compared with theory and the experimental results for the partial electron impact ionization of ground-state neon, Ne^{+}, of Krishnakumar and Srivastava (1988).

4. Results and discussion

Our results for the ionization cross sections of metastable neon are shown in figures 4–6. The results are absolute in that they have not been fitted to any other metastable data, but they do rely on the ground-state neon ionization data of Krishnakumar and Srivastava (1988). Any error in Krishnakumar and Srivastava's measurement will be reflected in our results. To estimate the possible effects this may have on our results we need to survey other ground-state measurements. While many measurements have been made, the five papers relevant to our experiment are Adamczyk *et al* (1966), Gaudin and Hagemann (1967), Stephan *et al* (1980), Wetzel *et al* (1987), and Krishnakumar and Srivastava. At 90 eV, Stephan *et al* and Wetzel *et al* differ from Krishnakumar and Srivastava by 2% and 5%, respectively, and the other measurements are within experimental error. Krishnakumar and Srivastava report that the relative shapes of cross sections for all five papers agree to within 10% over the energy range of interest. Any error introduced into our absolute scale and shape, by using Krishnakumar and Srivastava's ground-state data, is well within our reported error bars.

To take into account the spread in the impact energy, the results for each run were separately sorted into 1.8 eV wide bins. The bin width was governed by the emission properties of the electron gun cathode ($\pm$500 meV), space charge effects in the electron beam ($\pm$250 meV), electron and atomic beam collimation effects ($\pm$150 meV), and, to a far lesser extent, the velocity distribution of the atomic beam ($\pm$1.5 meV). For a single run at a given energy, the cross section is the average of all data in the bin with the statistical error being determined by the standard deviation of the data.

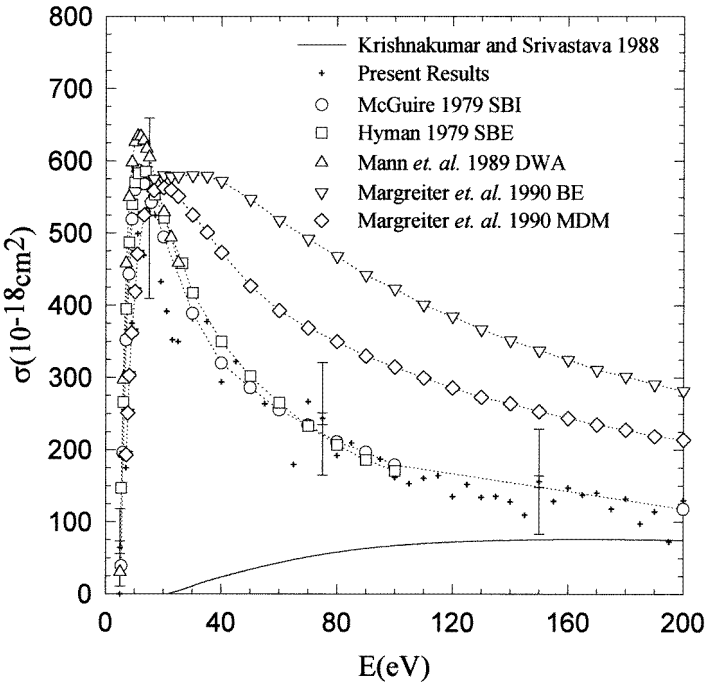

Figure 6. Present results for the partial electron impact ionization cross section of metastable neon, Ne^{*+}, compared with theory and the experimental results for the partial electron impact ionization of ground-state neon, Ne^{+}, of Krishnakumar and Srivastava (1988).

The systematic error was obtained when each run was independently placed on an absolute scale. The origin of the systematic error was the temperature measurements necessary for the determination of the secondary emission coefficients of the thermoelectric detector. While the absolute value of the ionization cross section had a relatively large systematic error, from run to run, the shape of the cross section curves were almost identical with a much smaller statistical error component. The reported cross section is an average of the separate runs weighted by their respective standard deviation. The total error, made up of both systematic and statistical components, is dominated by the systematic effects. Table 2 gives representative values for cross sections and the associated systematic and statistical errors.

The present results are compared with the unpublished experimental results of Dixon *et al* (1973) in figure 4 where it is seen that the general agreement, both in magnitude and in shape, is excellent. In fact the results agree so well that it must be re-emphasized that the two data sets are independent, and that our results have not been normalized to those of Dixon *et al*.

The theoretical calculation of the cross section for ionization of metastable neon are summarized in table 3. The ionization problem is difficult and many of the models find their roots in the classical model of Thomson (1912). Vriens (1964) used Gryzinski's model (Gryzinski 1959, 1965a, b, c) to calculate the ionization cross section for metastable neon from threshold to 80 eV. The results of Vriens' binary encounter calculations, which include both inner (2p) and outer shell contributions (BEI), are compared with the present results in figure 5. These calculations lie higher than the present results over most of the energy range.

Table 2. Representative ionization cross sections of metastable neon (Ne^{*+}): present results and error limits.

Energy (eV)	σ_m (10^{-18} cm^2)	± Statistical error (10^{-18} cm^2)	± Systematic error (10^{-18} cm^2)
4.92	0.0	—	—
5.0	64.4	8.7	45
7.0	175	45	200
9.0	375	30	160
11.0	499	14	150
13.0	469	9	130
15.0	534	10	115
17.0	525	16	110
19.0	433	12	100
21.0	392	11	90
23.0	352	9	95
25.0	350	6	90
30.0	382	7	80
40.0	294	8	75
50.0	305	7	75
75.0	243	8	70
100.0	162	9	70
125.0	152	13	65
150.0	156	8	65
200.0	130	11	70

Table 3. A summary of theoretical calculations for ionization of metastable neon by electron impact.

Reference	Theoretical approach	Energy range
Vriens (1964)	Semi-empirical	threshold–80 eV
Ton-That and Flannery (1977)	Semi-classical, Born	threshold–218 eV
McGuire (1979)	Scaled Born	threshold–1000 eV
Hyman (1979)	Semi-classical	threshold–100 eV
Mann *et al* (1989)	Distorted wave approximation	threshold–25 eV
Margreiter *et al* (1990)	Semi-classical, semi-empirical	threshold–200 eV

Figure 5 also shows the binary encounter and Born approximation calculations of Ton-That and Flannery (1977). Their Born half-range calculation (BHR) is in good agreement with our results, while, like the Vreins calculation, their binary encounter calculation including inner shell contributions appears to be somewhat high, Reasonable agreement exists with their Born full-range calculation (BFR) above 50 eV. Figure 6 compares the present results with the theoretical calculation of Hyman (1979), Margreiter *et al* (1990), McGuire (1979, 1977a, b) and Mann *et al* (1989). The results of Hyman, based on the symmetric binary encounter model (SBE) in which the indistinguishability of the incident and bound electrons is taken into account, the results of McGuire, based on a scaled Born approximation including inner shell contributions (SBI), and the results of Mann *et al* based on the distorted wave approximation (DWA) are in good agreement with the present results. The binary encounter (BE) and semi-empirical models (MDM) of Margreiter *et al* diverge from the present results above 20 eV.

5. Conclusions

The ionization cross sections of metastable neon by electron impact have been measured in the incident electron energy range of onset to 200 eV. The results are in good agreement with the unpublished experimental measurements of Dixon *et al* (1973). They are also in good agreement with the Born half-range calculation of Ton-That and Flannery (1977), the symmetric binary encounter calculation of Hyman (1979), the scaled Born calculations of McGuire (1979, 1977a, b), and the distorted wave approximation calculation of Mann *et al* (1989). The binary encounter calculations of Vriens (1964) and Ton-That and Flannery (1977), and the calculations of Margreiter *et al* (1990) all tend to be higher than the present results.

Acknowledgments

This work was supported by the joint Los Alamos, University of California, Riverside Campus, Laboratory Collaboration (CALCOR). The authors would like to acknowledge useful conversations with D C Cartwright, J B Mann, G Csanak, T J Gay and A D Khakhaev.

References

Adamczyk B, Boerboom A J H, Schram B L and Kistemaker J 1966 *J. Chem. Phys.* **44** 4640–2
Baum G, Fink M, Raith W, Steidl H and Taborski J 1989 *Phys. Rev.* A **40** 6734–6
Cartwright D 1993 Private communication
Chambers E S 1964 *Rev. Sci. Instrum.* **35** 95–7
Coggiola M J, Gaily T D, Gillen K T and Peterson J R 1979 *J. Chem. Phys.* **70** 2576–7
Csanak G, Cartwright D, Clark R and Abdallah J 1995 *48th Ann. Gaseous Electronics Conf. Full. Am. Phys. Soc. Series II* **40** 1546
Dixon A J, Harrison M F A and Smith A C H 1973 *VIII ICPEAC (Belgrade)* Abstracts, ed B C Cobic and M V Kurepa (Bristol: Institute of Physics) pp 405–6
——1976 *J. Phys. B: At. Mol. Phys.* **9** 2617–31
Dougherty J D, Mangano J A and Jacob J H 1976 *Appl. Phys. Lett.* **28** 581–3
Fite W L and Brackmann R T 1963 *Proc. VIth Int. Conf. on Ionization Phenomenon in Gases (Paris)* ed P Hubert
Gaudin A and Hagemann R 1967 *J. Chem. Phys.* **64** 1209–21
Gryzinski M 1959 *Phys. Rev.* **115** 374–83
——1965a *Phys. Rev.* **138** A305–21
——1965b *Phys. Rev.* **138** A322–35
——1965c *Phys. Rev.* **138** A336–58
Hyman H A 1979 *Phys. Rev.* A **20** 855–9
Jacob J H and Mangano J A 1976 *Appl. Phys. Lett.* **28** 724–6
Koller H H 1969 *Doctoral Thesis* University of Zürich
Krishnakumar E and Srivastava S K 1988 *J. Phys. B: At. Mol. Opt. Phys.* **21** 1055–82
Lin C C and Anderson L W 1991 *Advances in Atomic, Molecular and Optical Physics* vol 29, ed D Bates and B Bederson (New York: Academic) pp 1–32
Long D R and Geballe R 1970 *Phys. Rev.* A **1** 260–5
Lymberopoulos D P and Economou D J 1993 *J. Appl. Phys.* **73** 3668–79
Makabe T, Nakano N and Yamaguchi Y 1992 *Phys. Rev.* A **45** 2520–31
Mann J B, Merts A L and Csanak G 1989 Private communication
Margreiter D, Deutsch H and Märk T D 1990 *Contrib. Plasma Phys.* **30** 487–95
McGuire E J 1977a *Phys. Rev.* A **16** 62–72
——1977b *Phys. Rev.* A **16** 73–9
——1979 *Phys. Rev.* A **20** 445–56
Moore C E 1971 *Atomic Energy Levels Natl Bur. Stds* vols I, II, III (Washington, DC: US Government Printing Office)
Naynaber R H and Magnuson G D 1976 *J. Chem. Phys.* **65** 5239–41

Pierce J R 1954 *Theory and Design of Electron Beams* (New York: Van Nostrand)
Septier A (ed) 1967 *Focusing of Charged Particles* vol II (New York: Academic) pp 73–121
Shearer-Izumi W and Botter R 1974 *J. Phys. B: At. Mol. Phys.* **7** L125–8
Sommerer T J and Kushner M J 1992 *J. Appl. Phys.* **71** 1654–73
Stephan K, Helm H and Mark T D 1980 *J. Chem. Phys.* **73** 3763–78
Thomson J J 1912 *Phil. Mag.* **23** 449–57
Ton-That D and Flannery M R 1977 *Phys. Rev.* A **15** 517–26
Trajmar S and Nickel J C 1993 *Advances in Atomic, Molecular and Optical Physics* vol 30, ed D Bates and B Bederson (New York: Academic) pp 45–103
Vriens L 1964 *Phys. Lett.* **8** 260–1
Vriens L, Bonsen T F M and Smit J A 1968 *Physica* **40** 229–52
Wetzel R C, Baiocchi F A, Hayes T R and Freund R C 1987 *Phys. Rev.* A **35** 559–77